33. R. G. Bromley, in (*22*), p. 16.
33a. E. Voigt, *Leopoldina* **6**, 379 (1930); *Geologie* **8**, 1 (1959); *Ber. Dutsch. Ges. Geol. Wiss. Reihe A*, **12**, 479 (1967); *Bur. Rech. Géol. Min. Mém.* **77**, 45 (1972).
34. E. Håkansson and E. Thomsen, in (*22*), p. 78.
35. T. Birkelund and E. Håkansson, in (*22*), p. 373.
36. M. A. Nazarov *et al.*, *13th Lunar Planet. Sci. Conf.* (1982), p. 580.
37. E. Håkansson, personal communication.
38. F. Surlyk, thesis, University of Copenhagen (1969); *Bull. Geol. Soc. Den.* **20**, 152 (1970); *Newsl. Stratigr.* **1**, 7 (1970); *Biol. Skr. Dan. Vidensk. Selsk.* **19**, 1 (1972); *Bull. Geol. Soc. Den.* **22**, 219 (1973); *Palaeogeogr. Palaeoclimatol. Palaeoecol.* **15**, 185 (1974).
39. ______, in (*22*), p. 48
40. ______ and M. B. Johansen, *Abstr. 3rd Eur. Meet. Int. Assoc. Sedimentol.* (1982), p. 112.
41. M. B. Johansen, thesis, University of Copenhagen (1982).
42. F. Surlyk and M. B. Johansen, *Abstr. 148th Meet. AAAS* (1982), p. 49; *Science* **223**, 1174 (1984).
43. E. G. Kauffman and N. F. Sohl, in *Encyclopedia of Paleontology*, R. W. Fairbridge and D. Jablonski, Eds. (Dowden, Hutchinson & Ross, Stroudsburg, Pa., 1979), p. 723.
44. J. D. Taylor, W. J. Kennedy, A. Hall, *Bull. Br. Mus. (Natl. Hist.) Zool.* (Suppl. 3) (1969); W. J. Kennedy, J. D. Taylor, A. Hall, *Biol. Rev.* **44**, 499 (1969).
45. C. Heinberg, in (*22*), p. 58.
46. T. Birkelund and R. Bromley, in (*22*), p. 5.
47. W. J. Kennedy, N. J. Morris, J. D. Taylor, *Palaeontology* **13**, 379 (1970).
48. W. J. Kennedy and J. D. Taylor, *Proc. Geol. Soc. London, No. 1645* (1968), p. 325.
49. P. Gravesen, in (*22*), p. 8.
50. We thank P. D. Ward, P. W. Signor, and T. A. Hansen for helpful criticism. This work was supported by NSF grant EAR-81-15858.

Hydrogen-Evolving Solar Cells

Adam Heller

Summary. Sunlight is directly converted to chemical energy in hydrogen-evolving photoelectrochemical cells with semiconductor electrodes. Their Gibbs free energy efficiency of solar-to-hydrogen conversion, 13.3 percent, exceeds the solar-to-fuel conversion efficiency of green plants and approaches the solar-to-electrical conversion efficiency of the best *p–n* junction cells. In hydrogen-evolving photoelectrodes, electron-hole pairs photogenerated in the semiconductor are separated at electrical microcontacts between the semiconductor and group VIII metal catalyst islands. Conversion is efficient when the island diameters are small relative to the wavelengths of sunlight exciting the semiconductor; when the island spacings are smaller than the diffusion length of electrons at the semiconductor surface; when the height of the potential energy barriers that separate the photogenerated electrons from holes at the semiconductor surface is raised by hydrogen alloying of the islands; when radiationless recombination of electron-hole pairs at the semiconductor-solution interface between the islands is suppressed by controlling the semiconductor surface chemistry; and when the semiconductor has an appropriate band gap (1.0 to 1.8 electron volts) for efficient solar conversion.

Optimal conversion of sunlight by a single-threshold converter, whether semiconductor-based or molecular, requires an energy gap near 1.4 electron volts (*1–3*). Tandem systems, based on two semiconductors or on two light-harvesting molecules, require materials with gaps near 1.8 and 1.0 eV (*4*). At normal solar irradiance and at 27°C, the thermodynamic limit to the solar conversion efficiency is 27 percent for a single converter and 36 percent for tandem cells (*4*). For nonconcentrated sunlight the actual efficiency that has been attained is 21.9 percent (*5*). Although the thermodynamic efficiency limits for semiconductor and molecular systems are the same, all efficient systems today are semiconductor-based.

The foundations of the science of semiconductor-based photoelectrodes were laid between 1955 and 1970 (*6–16*). In 1972 it was shown that when an oxygen-evolving metal anode is replaced by the stable semiconducting anode *n*-TiO_2 (*17*), a substantial part of the electrical energy required for the electrolysis of water is conserved (*18*). Unfortunately, the band gap (E_{BG}) of *n*-TiO_2 is 3.0 eV, so the excitation spectrum of this material is confined to the ultraviolet. Consequently, sunlight could not be efficiently converted in early cells based on *n*-TiO_2 or *n*-$SrTiO_3$ (E_{BG} = 3.2 eV) photoanodes (*19–24*).

Photoanodes with band gaps appropriate for efficient solar conversion were first reported in 1960 (*9*), before the introduction of the concept of power-producing ("regenerative") cells (*25*). However, these were quite unstable. Ideas for their stabilization emerged in 1966 (*26*), but the introduction of relatively stable photoanodes took nearly a decade (*27–50*).

Simultaneously, the second key problem of photoelectrodes, the reduction of quantum yield from radiationless recombination of electron-hole pairs at the semiconductor-solution interface, was addressed. It was shown that recombination can be reduced by properly controlling the interfacial chemistry (*37, 51–66*). These advances led to the first power-producing photoelectrochemical cells of greater than 10 percent solar conversion efficiency (*51, 52, 63, 64, 67*). Stabilization and reduction of surface recombination also opened the way to efficient and direct photoelectrochemical cells for producing hydrogen. These cells are the subject of this article.

Photoelectrodes

Hydrogen can be evolved in either photocathode- or photoanode-based cells. Photocathodes and photoanodes are based on electrical contacts between semiconductors and electrolytes, between semiconductors and metallic electrocatalysts, or between semiconductors and both electrolytes and catalysts. Associated with these contacts is a barrier, ψ_B, which separates the photogenerated electrons (e^-) and holes (h^+) (Fig. 1). Hydrogen evolution at photocathodes requires the presence of a catalyst on or near the surface. When the catalyst is on the surface of the semiconductor, photogenerated electrons diffuse or drift to the interface of the semiconductor and the catalyst (Fig. 1a), where they reduce adsorbed protons to form hydrogen, according to $2e^- + 2H^+ \rightarrow H_2$. Electrical neutrality is maintained by transport of holes through both the bulk of the semiconductor and its back electrical contact to the anode, where they oxidize either dissolved anions such as chloride, through the reaction $2h^+ + 2Cl^- \rightarrow Cl_2$, or water itself, through the reaction

---

Adam Heller is a member of the technical staff and head of the Electronic Materials Research Department at Bell Laboratories, Murray Hill, New Jersey 07974.

$4h^+ + 2H_2O \rightarrow 4H^+ + O_2$. As in conventional solar cells, the light generates a potential difference between the front and the back of the semiconductor. If this photogenerated potential is inadequate to produce electrolysis, it must be augmented by an external d-c power source.

In illuminated photoanodes, the photogenerated holes drift to the contacting solution interface, where they oxidize the electrolyte or water. The electrons traverse the semiconductor to the back contact and reach the cathode through the external circuit, where they reduce protons to hydrogen (Fig. 1b).

If the Gibbs free energy change in a thermodynamically uphill reaction, such as $H_2O \rightarrow H_2 + 1/2\ O_2$, is ΔG kcal/mole, and if the same reaction can be run under sunlight by investing only $\Delta G'$ kcal/mole, the Gibbs free energy efficiency of solar-to-chemical conversion is $\eta = (\Delta G - \Delta G')/\int_0^\infty I\, d\lambda$, where the denominator is the solar irradiance (I) integrated over wavelengths from $\lambda = 0$ to $\lambda = \infty$. In an electrochemical cell a gain in free energy translates to a reduction in the potential bias needed for electrolysis. If electrolysis requires in a thermodynamically reversible cell a potential bias of $V = \Delta G/nF$ volts (where n is the number of electrons transferred and F is Faraday's constant), and if under sunlight electrolysis results at a bias $V' = \Delta G'/nF$, a bias reduction $\Delta V = V - V'$ is realized. The Gibbs free energy efficiency of solar-to-chemical conversion (η, Fig. 2) is now defined by

$$\eta = \frac{\Delta V_{\max} \cdot i_{\max}}{\int_0^\infty I\, d\lambda} \qquad (1)$$

where $\Delta V_{\max}$ and $i_{\max}$ are the reduction in potential bias and the photocurrent density at the point where their product reaches its maximum value. Thus η is 10 percent if, at pH 0, under a solar irradiance of 100 mW/cm^2 hydrogen is evolved at $\Delta V_{\max} = +0.5$ V versus the standard hydrogen electrode (SHE) potential, at a photocurrent density $i_{\max} = 20$ mA/cm^2. At the threshold of hydrogen evolution ($i = 0$), ΔV is ΔV_{oc}. At $\Delta V = 0$ the photocurrent density is i_{sc} (Fig. 2).

Quantum Efficiency

A photoelectrode reaches its theoretical integrated quantum efficiency of unity when all incident photons with energies exceeding E_{BG} produce electron-hole pairs and when all of the charge carriers react with the electrolytic solution to produce the desired cathodic and anodic products. Losses in current efficiency are caused by radiationless recombination of photogenerated electron-hole pairs, leakage of the "wrong" charge carriers across the barrier, absorption and reflection of photons by the metallic catalyst needed to accelerate the desired electrochemical reaction, reflection of photons at the semiconductor-solution interface, absorption of light by the solution, and undesired electrode reaction products.

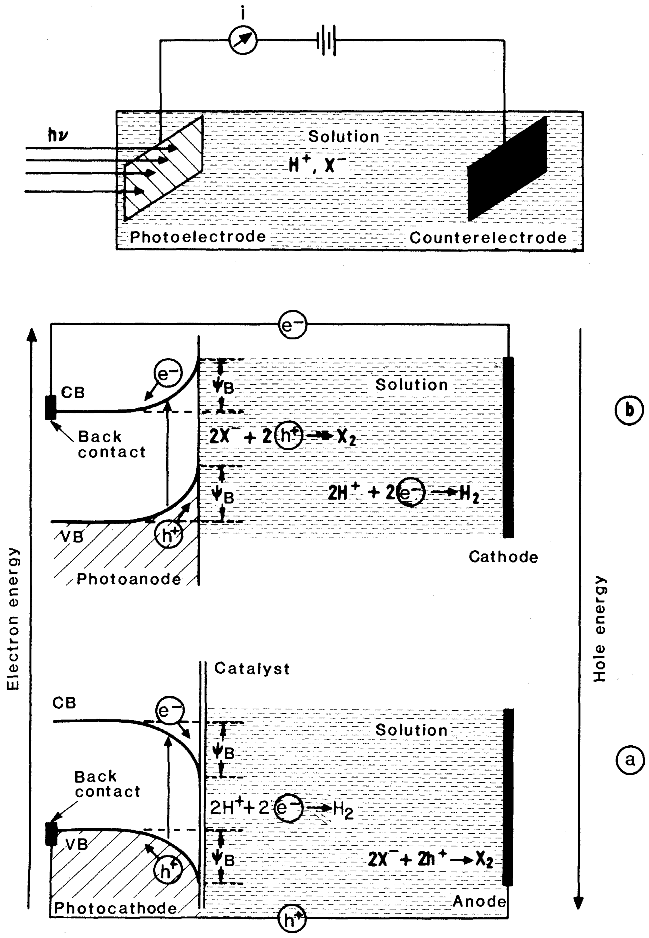

Fig. 1. (a) Separation, transport, and reaction of photogenerated electron-hole pairs in photocathode-based cells. Under intense irradiance the maximum bias reduction (ΔV_{oc}) approaches the height of the barrier that separates the charge carriers (ψ_B). (b) Same, in photoanode-based cells. Abbreviations: *CB*, conduction band; *VB*, valence band.

Recombination, leakage, and reflection losses are common to all solar cells (*1*). In hydrogen-generating cells the quantum efficiency is determined by the ratio of the desired rate of hydrogen evolution to the sum of this rate and the undesired recombination and leakage rates (*68*). All of these rates depend on ΔV and on the surface chemistry of the semiconductor. Hydrogen evolution at high ΔV is much slower on most semiconductor surfaces than are recombination and leakage, even if the latter are suppressed by a properly controlled interfacial chemistry. Hydrogen production is greatly enhanced when a group VIII metal catalyst, such as platinum, is incorporated in the semiconductor surface (*69*).

An example of a catalyst-caused change from recombination and leakage to efficient hydrogen production is seen in p-InP photocathodes (*69–72*), which have ideal band gaps for solar conversion (E_{BG} = 1.34 eV). In contact with aqueous acids, their surfaces become covered with a 6- to 10-Å pore-free layer of hydrated indium oxide, through which electrons freely tunnel (*73*). The thin indium oxide layer, together with cathodic protection by the photogenerated electrons (*69–72*), provides stability against oxidative corrosion (*74–75*). This layer also reduces ("passivates") the radiationless recombination of the photogenerated electrons with holes (*62, 64, 65, 71, 72*). The presence of a group VIII metal at the surface catalyzes the reaction $H^+ + e^- \rightarrow 1/2\ H_2$ and thereby increases the hydrogen evolution rate and the quantum efficiency. For example, at pH 0 and $\Delta V = 0.5$ V incorporation of platinum yields an increase in quantum efficiency of 10^4, to 0.8 (Fig. 3) (*72*).

A uniform, 50-Å-thick layer of platinum will, however, reflect and absorb about half the useful photons in the solar spectrum. To avoid much of this loss, the catalyst must be deposited in the form of islands with diameters smaller than the useful wavelengths of sunlight. Coverage of a semiconductor surface by such catalyst islands results in greater transmission of light than expected from simple geometric reasoning, because of the screening of the optical electric field by the mobile electronic charge of the metal. This screening channels the light into the regions between the islands. This phenomenon, well known in the study of the optical response of heterogeneous materials (*76*), is described by the effective medium theory (*77*).

While increasing the island spacing improves the optical efficiency, it also reduces the collection efficiency of photogenerated electrons. The crossover point occurs where nearly all the electrons reach the islands before recombining with holes or leaking through the barrier. The maximum acceptable spacing between the islands can be increased and the transmission of photons to the semiconductor improved by increasing the ratio of lateral diffusivity to recombination and leakage of the electrons. Therefore, the most efficient photoelectrodes for conversion of solar energy to hydrogen are made from high-quality, defect-free semiconductors with nonleaking barriers and with surface recombination passivated by a controlled semiconductor surface chemistry. If the surface diffusivity of electrons is small, one must choose between a severe light absorption loss caused by a high density of catalyst islands, or a severe loss in collection efficiency from a low density of catalyst islands. Thus, high quantum (current) efficiency can be achieved only when three conditions are simultaneously met: the catalyst islands cover only a small fraction of the surface; their diameter is much smaller than the wavelength of the exciting photons; and their spacing is not larger than the minority carrier surface diffusion length.

Two examples which demonstrate that catalyst islands smaller than the wavelength of exciting light do not reduce the quantum efficiency in proportion to their surface coverage are given in Fig. 4. In one (Fig. 4a) the platinum catalyst islands cause a loss of less than 8 percent in the quantum efficiency of the *p*-InP photocathode, even though the islands, with an average diameter of 700 Å, cover about 40 percent of the surface and are several hundred angstroms thick. The islands in Fig. 4b, with an average diameter of 1400 Å, are ~ 1000 Å high and cover 60 percent of the *p*-InP surface. However, the light absorption loss is less than 30 percent (*78*). Because the surface diffusion length of electrons in *p*-InP is much greater than the ~ 1000-Å spacing between the islands, all of the photogenerated electrons are collected efficiently.

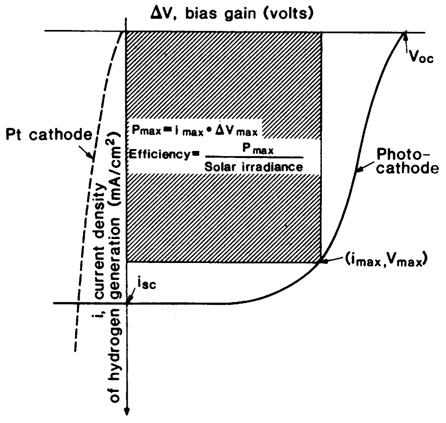

Fig. 2 (left). Definition of the maximum bias reduction (ΔV_{oc}), the short circuit current (i_{sc}), and the maximum solar-to-hydrogen conversion point (ΔV_{max}, i_{max}). The Gibbs free energy efficiency is the ratio of the product $\Delta V_{max} \cdot i_{max}$ to the solar irradiance integrated over all wavelengths.

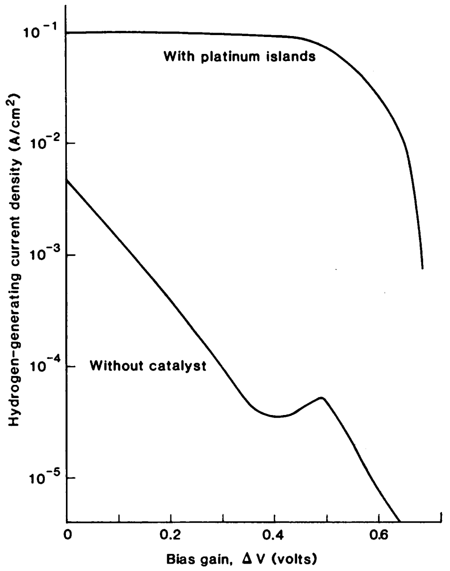

Fig. 3 (right). Increase of the current density of hydrogen evolution upon incorporation of platinum in the surface of a *p*-InP photocathode, as a function of ΔV ($3M$ $HClO_4$, tungsten-halogen source).

The surface chemistry, which determines the density and distribution of surface states in which photogenerated carriers recombine, is dependent on potential. Consequently, an island spacing that ensures efficient hydrogen generation at one potential may not be suitable at another. This is illustrated for catalyzed *p*-InP photocathodes. Their quantum efficiency drops at excessively reducing potentials or upon operation at low ΔV. The drop is caused by a partial loss of the indium oxide layer, which introduces recombination centers (*79*). Full efficiency is readily restored upon reoxidation of the surface (*69, 70, 72, 80*).

The photocurrent efficiency is a function of the surface composition also in photoanodes. Layered-compound photoanodes, such as *n*-$MoSe_2$ and *n*-WSe_2, have appropriate band gaps for solar conversion. They are more stable against oxidative photocorrosion than other photoanodes having such band gaps (*35, 40–43, 57, 59–61, 63, 67, 81, 82*), but stability and high current efficiency are realized only for the cleavage (van der Waals) planes of the crystals (*43, 57, 59–61, 63, 67, 82*). Because electron-hole recombination is rapid on the other crystallographic planes, the solar conversion efficiency decreases with the density and height of steps in the surface (Fig. 5) (*57, 59, 60*). With perfectly smooth photoanodes, efficiencies of 10 percent have been reached (*63, 67*).

Other than recombination, leakage is

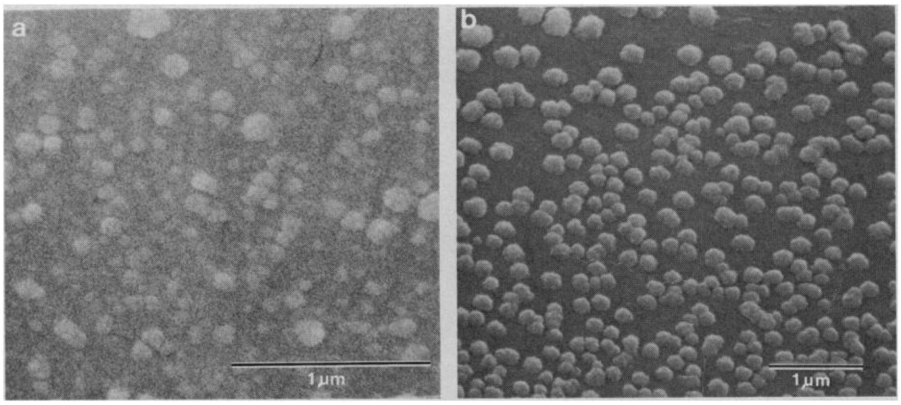

Fig. 4. Platinum islands on a hydrogen-evolving *p*-InP photocathode. The dimensions of the islands are small relative to the wavelengths of the solar spectrum exciting the semiconductor and are spaced at center-to-center distances smaller than the surface diffusion length of the photogenerated electrons. In (a) about 40 percent of the surface is covered with an optically thick catalyst layer, but fewer than 8 percent of the solar photons are lost. In (b) the optically thick catalyst covers 60 percent of the surface, but fewer than 30 percent of the photons are lost (*78*).

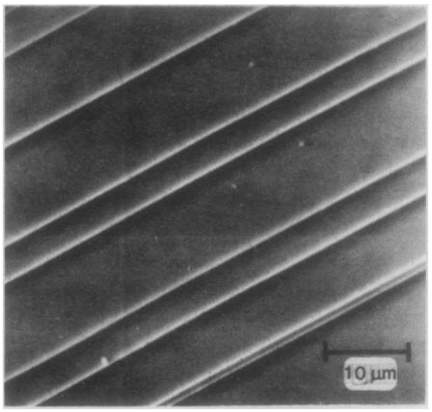

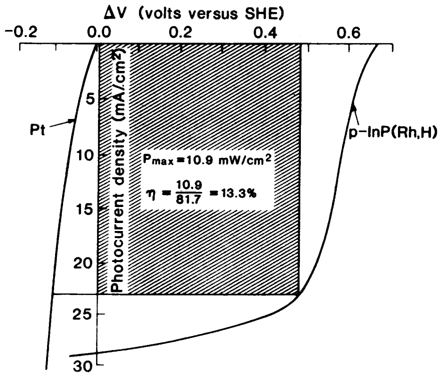

Fig. 5 (left). Electron beam–induced current micrograph of a p-WSe_2/Al contact. Light areas, representing sites where electrons and holes recombine, are observed at steps in the van der Waals plane. (*60*). Fig. 6 (right). Photocurrent bias reduction characteristics of a p-InP/(hydrogen-saturated rhodium) photocathode in 1*M* $HClO_4$ under sunlight at 81.7 mW/cm². The solar-to-hydrogen conversion efficiency is 13.3 percent (*80*).

the most important loss process. Leakage of majority carriers (holes in photocathodes and electrons in photoanodes) from the bulk of the semiconductor to the catalyst or to the solution interface reverses the desired photoelectrochemical reaction. Leakage of minority carriers (electrons in photocathodes and holes in photoanodes) from the catalyst, or from the solution interface, to the bulk produces the same effect. If interfacial hydrogen atoms are oxidized either by bulk holes or by loss of electrons to the bulk, the quantum efficiency of hydrogen evolution drops.

Leakage is caused by thermionic emission across, or by chemical imperfections in, the barrier (ψ_B) that separates the photogenerated minority and majority carriers (Fig. 1). It is avoided if the interfacial potential barrier is made uniformly high. For example, metallic ruthenium forms a leaky barrier with n-GaAs. The leakage is reduced when the metal is saturated with hydrogen that reacts with the leakage-causing sites (*83*).

Bias Reduction

In a hydrogen-evolving solar cell, the bias reduction (ΔV) is the equivalent of the photovoltage in a power-generating cell. Like the open-circuit photovoltage (V_{oc}) of a power-generating cell, ΔV_{oc}, the bias reduction at the threshold for hydrogen generation is determined by the barrier height (ψ_B) and by the irradiance. In photocathode-based cells the contact that determines ψ_B is created between the semiconductor and the metal, not between the semiconductor and the solution. This is true even if only a small part of the surface of a hydrogen-generating photocathode is covered by the metal catalyst (*72*). The reason is that the overwhelming majority of the charge carriers reach the solution via the catalyst. The rate or current of hydrogen generation at the semiconductor-solution interface is usually negligible. Thus, catalyzed photoelectrodes that generate hydrogen are in essence classical metal-semiconductor or Schottky junctions. Their barriers are the same whether the cells are wet or dry (*72, 84*). In the absence of chemical reactions between the catalyst and the semiconductor, ψ_B depends on the catalyst work function (ϕ_w). In photocathodes, ψ_B increases when ϕ_w decreases; in photoanodes the reverse is true.

In some cases, the barrier height varies at different points of the semiconductor surface. The resulting leakage lowers the efficiency, unless the surface regions where the current might leak are covered by an electrical insulator or by a layer that blocks the transport of ions to and from the surface. Thus, there are three ways to reduce leakage losses: electrical insulation of the leakage sites; blockage of reactant transport to, or product transport from, the sites (for example, by a polymer layer); and maintenance of uniformly high barriers across the semiconductor surface. The last method is implemented in hydrogen-generating p-InP photocathodes, where the same V_{oc} is observed when hydrogen is adsorbed on the semiconductor surface, regardless of whether it is catalyst-covered or bare (*72*). In oxygen-evolving photoanodes, such as silicon with platinum-silicide islands (*85*), leakage is probably reduced by an insulating SiO_2 layer covering the nonmetallized regions between the islands.

Table 1. Barrier heights of catalyst contacts to semiconductors in air and in hydrogen.

Semiconductor	Catalyst	Barrier in air (eV)	Barrier in hydrogen (eV)
n-TiO_2	Pt	$\gtrsim 0.5$	0
	Rh	$\gtrsim 0.6$	0
	Ru	$\gtrsim 0.1$	0
n-$SrTiO_3$	Pt	$\gtrsim 0.6$	$\gtrsim 0.1$
	Rh	$\gtrsim 1.0$	$\gtrsim 0.1$
	Ru	$\gtrsim 0.7$	$\gtrsim 0.2$
n-CdS	Pt	1.84	1.63
	Rh	1.00	0.75
	Ru	1.28	0.75
p-InP	Pt	−0.72	−0.91
	Rh	−0.31	−0.81
	Ru	−0.57	−0.85

Dissolution of gases in catalysts and adsorption of gases on catalyst surfaces cause drastic changes in ϕ_w and therefore in ψ_B. Hydrogen dissolution in platinum, palladium, rhodium, rhenium, and ruthenium lowers ϕ_w, increasing ψ_B and ΔV_{oc} and thereby increasing the solar-to-hydrogen conversion efficiency of photocathodes (*72, 84*). These are decreased correspondingly in photoanodes. Thus, a catalyzed hydrogen-generating photocathode is most efficient when it is enveloped by hydrogen; a catalyzed oxygen- or halogen-evolving photoanode is most efficient when its products reactively eliminate traces of hydrogen from the catalyst. Values of ψ_B in air and in hydrogen (*84*) are listed in Table 1 for 12 semiconductor-catalyst contacts. While in 11 cases ψ_B is drastically different in air and in hydrogen, in CdS with platinum the change is minor. The reason for the small change is that platinum reacts with CdS to form a platinum sulfide. Thus the contact is not Pt/CdS, but a hydrogen-insensitive contact (PtS_x-Cd-CdS)/CdS.

In the absence of leakage and recombination, each tenfold increase in irradiance increases ΔV_{oc} by 59 mV until ΔV_{oc} approaches ψ_B. The photocathode p-InP/(hydrogen-saturated platinum) shows such ideal behavior (*72, 86*).

Efficient Hydrogen-Evolving Photocathodes

From the preceding sections it is evident that solar-to-hydrogen conversion can be efficient only if several requirements are simultaneously met. These include the classical requirements of all semiconductor-based converters, such as an appropriate band gap and an adequate minority carrier diffusion length, as well as requirements unique to hydrogen-generating photoelectrodes, such as chemical passivation of corrosion and photocorrosion reactions; acceleration of the hydrogen evolution kinetics by catalyst islands that are small relative to the wavelength of the exciting sunlight; distribution of these islands at distances smaller than the minority carrier surface diffusion length; and nonleaking, high barriers at the catalyst-semiconductor contacts.

Although numerous photocathodes have been explored, only catalyzed *p*-InP meets all the requirements, and it is the only photocathode now known that converts solar energy to chemical energy stored in hydrogen gas at a Gibbs free energy efficiency of 13.3 percent (*80*). Nevertheless, some of the less efficient photocathodes have interesting features. In *p*-$LuRhO_3$, an external catalyst is not needed (*87*); in another, *p*-type iron (magnesium) oxide has been used (*88*); in a third, based on *p*-Si, the catalyst has been placed in a polymer in contact with the semiconductor rather than directly on it (*89*).

The *i*-ΔV characteristics of the *p*-InP/(hydrogen-saturated rhodium) hydrogen-evolving photocathode under sunlight at 81.7 mW/cm^2 are shown in Fig. 6. The maximum reduction in bias at threshold for hydrogen evolution (ΔV_{oc}), is 0.64 V, and the quantum or current efficiency at $\Delta V = 0$ is ~ 0.9. The maximum solar-to-fuel conversion efficiency point is at $i_{max} = 23$ mA/cm^2 and $\Delta V_{max} = 0.45$ V, where the Gibbs free energy efficiency of solar-to-hydrogen conversion reaches 13.3 percent (*80*).

Efficient Photoanodes

In photoanode-based cells hydrogen is evolved at their nonilluminated, catalyst-activated counterelectrodes. The requirements that must be met for the cells to be efficient—particularly those related to electron-hole recombination, leakage, and barrier heights—apply equally to photocathodes and photoanodes. The catalyst requirements are, however, relaxed as some photoanodes function adequately in the absence of a metallic catalyst on their surface. For example, the oxidation of S^{2-} to S_2^{2-} (*22–29, 90*) and that of cysteine to cystine (*90, 91*) proceed on "bare" *n*-CdS at sufficient rates. Similarly, water is oxidized to oxygen on noncatalyzed *n*-TiO_2 (*12*), *n*-$SrTiO_3$ (*92–96*), *n*-WO_3 (*97*), and *n*-Fe_2O_3 (*98*). Nevertheless, oxygen- and chlorine-evolving *n*-Si photoanodes do require catalysts: Examples of catalyzed electrodes are *n*-Si/platinum silicide (*85*) and *n*-Si/indium tin oxide/RuO_2 (*99*).

The delicate relationship between the

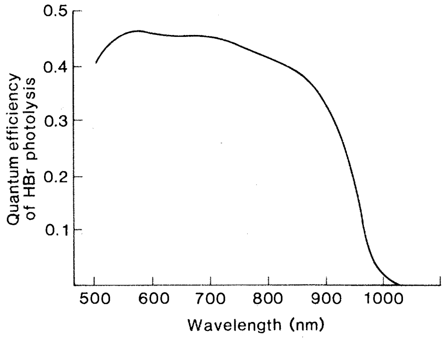

Fig. 7. Action spectrum for unassisted photoelectrolysis of aqueous HBr in the *p*-InP(Pt)/(2*M* HBr)/*n*-WSe_2 cell (*107*).

need for a catalyst and recombination is best seen in layered chalcogenide photoanodes like MoS_2, $MoSe_2$, WS_2, and WSe_2, on which I^- is oxidized to I_2 and I_3^-, Br^- to Br_2 and Br_3^-, and Cl^- to Cl_2. Because recombination of photogenerated electron-hole pairs is much more rapid on crystal faces perpendicular to the van der Waals planes than in the van der Waals planes themselves, a high ΔV can be reached, in the absence of a catalyst, only with perfectly smooth van der Waals surfaces (*63, 67*). However, if there is a high density of steps in these surfaces, then ΔV is small and is increased to values approaching those of smooth surfaces by incorporating platinum islands in the surface (*100*).

So far, most photoanodes of greater than 10 percent efficiency were made for and evaluated in electrical power producing cells (*65*). Among the photoanodes that were operated in electrolytic cells, *n*-$MoSe_2$, *n*-WSe_2 (*63, 67*), and Pt-catalyzed *n*-Si (*101*) were shown to produce a sufficient ΔV for the spontaneous photoelectrolysis of HI.

Two-Photoelectrode Cells

Splitting the incident sunlight between a photoanode and a photocathode connected by an electrolytic solution has two potential advantages. First, the sum of the two ΔV's is obtained, and the unassisted photoelectrolysis of species that cannot be photoelectrolyzed spontaneously in single-photoelectrode cells becomes possible (*102–104*). Second, different segments of the solar spectrum can be used for each of the two photoelectrodes and the solar conversion efficiency can be increased. As pointed out in the introduction, optimal efficiency is reached in two semiconductor systems when one semiconductor has a band gap of about 1.0 eV and the second about 1.8 eV (*4*).

For a two-photoelectrode cell to be efficient, the photocurrents of the two electrodes must be the same. This requires precise balancing of the spectral segments of sunlight that reach each of the electrodes and necessitates a system of a complexity substantially beyond that of present photoelectrochemical cells. For this reason, no optimized photoelectrochemical cell utilizing split segments of the solar spectrum has been reported. Furthermore, although many two-photoelectrode cells have been described since the introduction of the concept (*102–107*), only a few have both a photoanode and a photocathode with band gaps appropriate for solar conversion. Those that do have such gaps contain either an *n*-$MoSe_2$ or an *n*-WSe_2 photoanode and either a *p*-InP(Pt) or a *p*-InP(Rh) photocathode (*107*) and can photoelectrolyze aqueous HBr to H_2 and Br_2 and Br_3^- without an external bias. Their

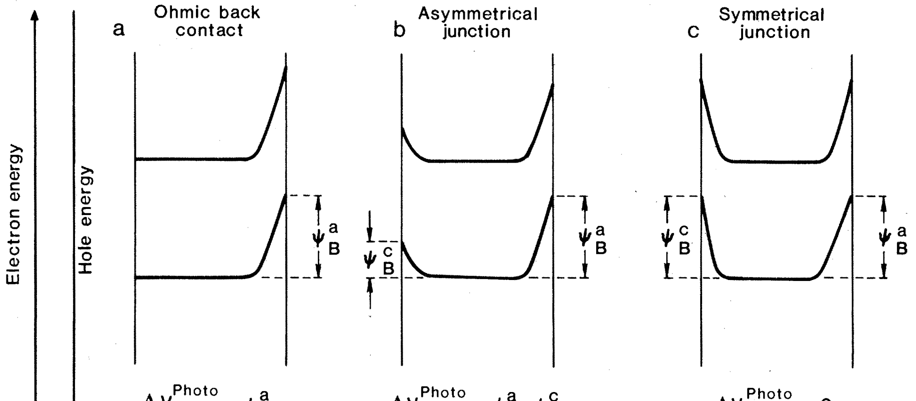

Fig. 8. Maximum bias gain in photoelectrolysis. The limit to ΔV_{oc} in a microcell consisting of a suspended semiconductor particle is the difference between the barrier height at the microcathode ($\psi_B{}^c$) and the barrier height at the microanode ($\psi_B{}^a$). (a) In an *n*-type semiconductor based cell with an ohmic microcathode contact, ΔV_{oc} equals the microanode barrier height. (b) In an asymmetric cell, more energy is gained in the transport of holes to the microanode than is lost in the transport of electrons to the microcathode. (c) In a symmetrical cell, all the anode gain is lost at the cathode and there is no net reduction in bias.

action spectra (Fig. 7) overlap the visible and near-infrared segments of the solar spectrum. If optimized, the cells should approach the Gibbs free energy efficiency of their individual photoelectrodes (~10 percent).

p-n Junction Cells

The classical *p-n* junction silicon solar cell (*108*) in which all the requirements for efficiency are met develops a sufficient photovoltage to electrolyze HI to H_2 and I_3^- (*109*). The photovoltage of a pair of *n-p* and *p-n* cells connected in series is adequate to electrolyze HBr to H_2 and Br_2/Br_3^- (*110, 111*). To accelerate the rate of hydrogen evolution at the SiO_2 layer of the Si-solution interface, and to generate conductive paths through the insulating SiO_2 layer that forms upon exposure of silicon to aqueous bromine, catalysts are incorporated in the solution-exposed surfaces of both the photocathode and the photoanode. The catalyst must not form metal-semiconductor contacts with barriers that impede electron transport to the cathode catalyst or hole transport to the anode catalyst.

The only commercial product-oriented engineering attempt at electrochemical solar cells in the United States utilized a pair of silicon *p-n* and *n-p* junctions. These were produced in the form of glass-embedded, etched, and catalyzed microspheres, which electrolyzed HBr. Photoelectrochemically formed hydrogen was stored as a metal hydride. When electric power was needed the products were allowed to recombine in a fuel cell (*110, 111*). The Gibbs free energy efficiency of the H_2- and Br_2-generating solar panels was 8.6 percent. Similar efficiencies have been reached in laboratory experiments on HI electrolysis with catalyzed *p-n* junctions (*109*).

Photoelectrolysis by Suspended Semiconductor Particles

Illuminated semiconductor particles suspended in a solution constitute a collection of microcells. The surface of each particle contains two chemically and physically distinct zones: a microanode and a microcathode.

The suspensions that have been explored thus far are of *n*-type particles. The analysis of the photoanode requirements applies to these, though with some modifications. Because the distances traversed by photogenerated charge carriers on their way to the microelectrodes are short, recombination in bulk impurity and defect centers is less important. Surface processes, including recombination, leakage, and electrochemical kinetics, dominate the characteristics. Surface recombination velocities decrease approximately exponentially with E_{BG}. The three semiconductors used thus far, *n*-TiO_2 (*112–116*), *n*-$SrTiO_3$ (*117, 118*), and *n*-CdS (*90–92, 119–121*), have large band gaps (3.0, 3.2, and 2.4 eV, respectively). While the large band gaps reduce recombination, they also rule out the possibility of attaining high solar conversion efficiencies. In very small particles (50 Å in diameter or less) the band gaps increase beyond their normal bulk value (*122*), further lowering the efficiency of the suspensions.

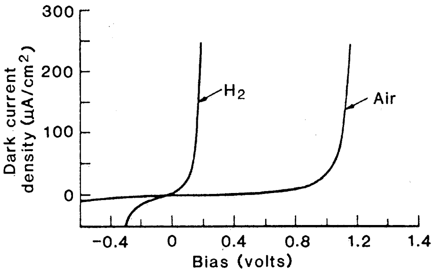

Fig. 9. Characteristics of the *n*-$SrTiO_3$/Rh contact in air and in hydrogen (*84*).

The fundamental requirement for photoelectrolysis by a microcell is

$$|\Delta V| > \frac{|\Delta G|}{nF} \qquad (2)$$

where ΔG is the Gibbs free energy of formation of the photoelectrolyzed species from the electrolytic reaction products. ΔV_{oc}, and therefore ΔV, is determined in the microcell by the difference between the barrier height at the microanode ($\psi_B{}^a$) and that at the microcathode ($\psi_B{}^c$) (Fig. 8). At very high irradiance

$$|\Delta V_{oc}| \rightarrow |\psi_B{}^a - \psi_B{}^c| \qquad (3)$$

When the anode and cathode barriers are equal in height, light cannot be converted to chemical energy (Fig. 8c). Any work gained upon transport of a hole to the microanode must be reinvested in the transport of an electron, across a blocking barrier, to the microcathode. The best microcells have microcathodes that are ohmic ($\psi_B{}^c = 0$) (Fig. 8a). The formation of ohmic microcontacts, a science in itself, is a formidable problem in suspended semiconductor particles, where ohmic contacts must be formed at some spots while high barrier contacts must be maintained at others. Fortunately, different microelectrode environments created by the chemical products of the microanode and microcathode reactions enhance the asymmetry (*84*).

The thermodynamic asymmetry requirement for the photoelectrolysis of water is

$$|\psi_B{}^a - \psi_B{}^c| \geq 1.23 \text{ eV} \qquad (4)$$

When group VIII metal–hydrogen evolution catalysts such as platinum are used, part or all of the asymmetry derives from hydrogen alloying of the catalyst at microcathode sites. As discussed earlier, and as seen in Table 1, hydrogen dissolution lowers the work function of the catalyst, decreasing the barrier heights of its contacts with *n*-type semiconductors and increasing the barrier heights with *p*-type semiconductors. Figure 9 shows an example of the reversible change in the diode characteristics of the Rh/*n*-$SrTiO_3$ Schottky diode in air and in hydrogen. While in air, the contact has a high barrier and is rectifying; it shows nearly ohmic behavior in hydrogen. The asymmetry of the barriers in the two environments is adequate to allow the Rh/*n*-$SrTiO_3$ contact to photoelectrolyze water. Note that hydrogen-saturated catalysts form microcathodes, while O_2-exposed catalysts form microanodes (*84*).

The likelihood of photoelectrolyzing water diminishes as the band gap of the semiconductor particles approaches the domain that is relevant for solar conversion, because ψ_B is always smaller than E_{BG}. Nevertheless, substrates that are less stable than water (Eqs. 2 and 3) might be photoelectrolyzed by particles with appropriate band gaps for solar conversion. For example, the free energy of formation of H_2S is much smaller than that of water. The asymmetry requirement can be relaxed to 0.14 eV (Eq. 3), at a penalty of reducing the amount of stored chemical energy from 1.23 to 0.14 eV per hydrogen atom. Indeed, photoelectrolysis of H_2S proceeds at high quantum yield on catalyzed *n*-CdS microcrystals (*121*) and might also proceed efficiently on microcrystals of materials with smaller gaps.

Because none of the suspensions as yet meet the essential band gap requirement, their solar-to-fuel conversion efficiencies remain low. The challenge is to find a system where $|\psi_B{}^a - \psi_B{}^c|$ is high enough to drive a substantially thermodynamically uphill reaction, where E_{BG} is in the range 1.0 to 1.7 eV, where the recombination velocity of the photogenerated electrons and holes at the semiconductor surface is lower than their rate of reaction with the electrolyte, and where the chemical and photochemical corrosion stabilities are adequate. Until such a system is found, efficient solar-to-hydrogen conversion will continue to require macroscopic photoelectrodes.

Conclusion

For efficient solar-to-hydrogen conversion, the photogenerated charge carrier reaction rates must be high relative to the rates of recombination and of leakage across the barrier. Conversion is efficient only under the following conditions: when electron-hole recombination at photoelectrode surface regions between the catalyst islands is slowed by a controlled interfacial chemistry, when an appropriate electrocatalyst accelerates hydrogen evolution, and when the chemistries of the semiconductor-catalyst and semiconductor-solution interfaces are such that the barrier separating the photogenerated electron and hole is uniformly high or such that no current can flow through low-barrier regions.

To avoid light absorption losses, the catalyst must cover only a fraction of the semiconductor surface and must form islands with diameters small relative to wavelengths of the solar spectrum exciting the semiconductor. To ensure efficient collection of the photogenerated charge carriers, these islands must be spaced at distances smaller than the surface diffusion length of the minority carriers.

Unassisted ("spontaneous") but inefficient solar photoelectrolysis of water is possible with large-band-gap semiconductor photoelectrodes or with microcells based on suspended, large-band-gap semiconductor particles. The photovoltage (ΔV), and thus the very feasibility of photoelectrolysis by a suspended particle, depends on the asymmetry of its microcathode and microanode barriers—that is, on the difference in the work functions of the cathode- and anode-forming catalysts. This difference is greatly enhanced by, and in some cases is entirely due to, a combination of hydrogen saturation of the microcathode and oxidative stripping of all traces of hydrogen from the microanode.

The barrier height is increased and the external voltage bias required for electrolysis is reduced in macroscopic, catalyzed photocathodes upon hydrogen saturation of the catalyst. In all of the efficient photoelectrodes ΔV is sufficient to allow unassisted solar electrolysis of HI. By pairing a photocathode with a photoanode, or a *p-n* junction with an *n-p* junction, HBr can also be spontaneously and efficiently photoelectrolyzed with sunlight. Although efficient solar electrolysis of HCl or water requires an external bias, a substantial part of the energy consumed in the generation of either hydrogen and chlorine or hydrogen and oxygen can now be derived from sunlight.

References and Notes

1. S. J. Fonash, *Solar Cell Device Physics* (Academic Press, New York, 1981), p. 127.
2. M. Almgren, *Photochem. Photobiol.* **27**, 603 (1978).
3. G. Porter, *J. Chem. Soc. Faraday Trans. 2* **79**, 473 (1983).
4. J. C. C. Fan, B. Y. Tsaur, B. J. Palm, *Proc. 16th IEEE Photovoltaic Specialists Conf.* (September 1982), p. 692.
5. J. M. Woodall and H. J. Hovel, *Appl. Phys. Lett.* **30**, 492 (1977).
6. W. H. Brattain and G. C. B. Garrett, *Phys. Rev.* **99**, 376 (1955).
7. J. F. Dewald, *Bell Syst. Tech. J.* **39**, 615 (1960).
8. M. Green, in *Modern Aspects of Electrochemistry*, J. O'M. Bockris, Ed. (Academic Press, New York, 1959), p. 343.
9. R. Williams, *J. Chem. Phys.* **32**, 1505 (1960).
10. H. Gerischer, in *Advances in Electrochemistry and Electrochemical Engineering*, P. Delahay, Ed. (Interscience, New York, 1961), p. 139.
11. Yu. V. Pleskov and V. A. Tyagai, *Dokl. Akad. Nauk. SSSR* **141**, 1135 (1961).
12. P. J. Boddy, *J. Electroanal. Chem.* **10**, 199 (1965).
13. R. Memming and G. Schwandt, *Angew. Chem. Int. Ed. Engl.* **6**, 851 (1967).
14. V. A. Myamlin and Yu. V. Pleskov, *Electrochemistry of Semiconductors* (Plenum, New York, 1967).
15. W. Gomes and F. Cardon, *Ber. Bunsenges. Phys. Chem.* **74**, 431 (1970).
16. H. Gerischer, in *Physical Chemistry: An Advanced Treatise*, vol. 9A, *Electrochemistry*, H. Eyring, D. Henderson, W. Jost, Eds. (Academic Press, New York, 1970), p. 463.
17. P. Boddy, *J. Electrochem. Soc.* **115**, 199 (1968).
18. A. Fujishima and K. Honda, *Nature (London)* **238**, 37 (1972).
19. H. Gerischer, *Top. Appl. Phys.* **31**, 115 (1979).
20. A. J. Nozik, *Adv. Hydrogen Energy: Hydrogen Energy Syst.* **3**, 1217 (1979).
21. L. A. Harris and R. H. Wilson, *Annu. Rev. Mater. Sci.* **8**, 99 (1978).
22. M. Tomkiewicz and H. Fay, *Appl. Phys.* **18**, 1 (1979).
23. M. A. Butler and D. S. Ginley, *J. Mater. Sci.* **15**, 1 (1980).
24. A. J. Bard, *Science* **207**, 4427 (1980).
25. H. Gerischer, *J. Electroanal. Chem.* **58**, 263 (1975).
26. G. C. Barker, discussing paper by H. Gerischer, *J. Electrochem. Soc.* **113**, 1182 (1966).
27. A. B. Ellis, S. W. Kaiser, J. M. Bolts, M. Wrighton, *J. Am. Chem. Soc.* **98**, 1635 (1976).
28. G. Hodes, J. Manassen, D. Cahen, *Nature (London)* **260**, 312 (1976); *ibid.* **261**, 403 (1976).
29. B. Miller and A. Heller, *ibid.* **262**, 680 (1976).
30. A. Heller, Ed., *Semiconductor–Liquid Junction Solar Cells* (Electrochemical Society, Princeton, N.J., 1977).
31. K. C. Chang, A. Heller, B. Schwartz, S. Menezes, B. Miller, in (*30*), p. 132; *Science* **196**, 1097 (1977).
32. H. Gerischer, in (*30*), p. 1; *J. Electroanal. Chem.* **82**, 133 (1977).
33. A. J. Bard and M. S. Wrighton, *J. Electrochem. Soc.* **124**, 1706 (1977).
34. A. B. Ellis, J. M. Bolts, S. W. Kaiser, M. S. Wrighton, *J. Am. Chem. Soc.* **99**, 2848 (1977).
35. H. Tributsch, *Z. Naturforsch. Teil A* **32**, 972 (1977); *Ber. Bunsenges. Phys. Chem.* **81**, 361 (1977).
36. B. Miller, S. Menezes, A. Heller, in (*30*), p. 186.
37. A. Heller and B. Miller, *Adv. Chem. Ser.* **184**, 215 (1980).
38. A. Heller, K. C. Chang, B. Miller, *J. Am. Chem. Soc.* **100**, 684 (1978).
39. A. Heller, G. P. Schwartz, R. G. Vadimsky, S. Menezes, B. Miller, *J. Electrochem. Soc.* **125**, 1156 (1978).
40. H. Tributsch, *ibid.*, p. 1086.
41. J. Gobrecht, H. Gerischer, H. Tributsch, *Ber. Bunsenges. Phys. Chem.* **82**, 1331 (1978); see also S. Menezes, F. J. DiSalvo, B. Miller, *J. Electrochem. Soc.* **127**, 1751 (1980).
42. J. Gobrecht, H. Tributsch, H. Gerischer, *J. Electrochem. Soc.* **125**, 2085 (1978).
43. W. Kautek, H. Gerischer, H. Tributsch, *Ber. Bunsenges. Phys. Chem.* **83**, 1000 (1979).
44. B. Miller, S. Menezes, A. Heller, *J. Electrochem. Soc.* **126**, 1483 (1979).
45. S. Menezes, A. Heller, B. Miller, *ibid.* **127**, 1263 (1980).
46. H. Gerischer, *Faraday Discuss. Chem. Soc.* **70**, 137 (1980).
47. F. Cardon, W. P. Gomes, F. Vanden Kerchove, D. Van Mackelbergh, F. Van Overmeire, *ibid.*, p. 153.
48. B. Miller, A. Heller, S. Menezes, H. J. Lewerenz, *ibid.*, p. 223.
49. K. W. Frese, Jr., M. S. Madou, S. R. Morrison, *J. Phys. Chem.* **84**, 3172 (1980); *J. Electrochem. Soc.* **128**, 1527 (1981); *ibid.*, p. 1939.
50. D. Cahen, G. Hodes, J. Manassen, R. Tenne, *Am. Chem. Soc. Symp. Ser.* **146**, 369 (1981).
51. A. Heller, B. A. Parkinson, B. Miller, *Proc. 13th IEEE Photovoltaic Specialists Conf.* (1978), p. 1253.
52. B. A. Parkinson, A. Heller, B. Miller, *Appl. Phys. Lett.* **33**, 521 (1978).
53. A. Heller, K. C. Chang, B. Miller, *J. Am. Chem. Soc.* **100**, 684 (1978).
54. B. A. Parkinson, A. Heller, B. Miller, *J. Electrochem. Soc.* **126**, 954 (1979).
55. A. Heller, H. J. Lewerenz, B. Miller, *Ber. Bunsenges. Phys. Chem.* **84**, 592 (1980).
56. R. J. Nelson *et al.*, *Appl. Phys. Lett.* **36**, 76 (1981).
57. H. J. Lewerenz, A. Heller, F. J. DiSalvo, *J. Am. Chem. Soc.* **102**, 1877 (1980).
58. A. Heller and B. Miller, *Electrochim. Acta* **25**, 29 (1980).
59. A. Heller, *Am. Chem. Soc. Symp. Ser.* **146**, 57 (1981).
60. H. J. Lewerenz, A. Heller, H. J. Leamy, S. D. Ferris, *ibid.*, p. 17.
61. H. Gerischer, *ibid.*, p. 1.
62. A. Heller, B. Miller, H. J. Lewerenz, K. J. Bachmann, *J. Am. Chem. Soc.* **102**, 6555 (1980).
63. B. A. Parkinson, T. E. Furtak, D. Canfield, K. Kam, G. Kline, *Faraday Discuss. Chem. Soc.* **70**, 233 (1980).
64. A. Heller, B. Miller, F. A. Thiel, *Appl. Phys. Lett.* **38**, 282 (1981).
65. A. Heller, *Acc. Chem. Res.* **14**, 154 (1981).
66. ———, H. J. Lewerenz, B. Miller, *J. Am. Chem. Soc.* **103**, 200 (1981).
67. G. Kline, K. Kam, D. Canfield, B. Parkinson, *Sol. Energy Mater.* **4**, 301 (1981); B. A. Parkinson, *J. Chem. Educ.* **60**, 338 (1983).
68. A. Heller, in *Energy Resources by Photochemistry and Catalysis*, M. Grätzel, Ed. (Academic Press, New York, 1983), p. 385.
69. ——— and R. G. Vadimsky, *Phys. Rev. Lett.* **46**, 1153 (1981).
70. A. Heller, *Sol. Energy* **29**, 153 (1982).
71. ———, in *Photochemical Conversion and Storage of Solar Energy*, J. Rabani, Ed. (Weizmann Science Press, Jerusalem, 1982), part A, p. 63.
72. A. Heller, E. Aharon-Shalom, W. A. Bonner, B. Miller, *J. Am. Chem. Soc.* **104**, 6942 (1982).
73. H. J. Lewerenz, D. E. Aspnes, B. Miller, D. L. Malm, A. Heller, *ibid.*, p. 3325.
74. L. F. Schneemeyer and B. Miller, *J. Electrochem. Soc.* **129**, 1977 (1982).
75. S. Menezes, B. Miller, K. J. Bachmann, *J. Vac. Sci. Technol.* **B1**, 48 (1983).
76. D. E. Aspnes, *Thin Solid Films* **89**, 249 (1982).
77. D. A. G. Bruggeman, *Ann. Phys (Leipzig)* **24**, 636 (1935); *ibid.*, p. 665; *ibid.* **25**, 645 (1936).
78. A. Heller and R. G. Vadimsky, unpublished results.
79. E. Aharon-Shalom and A. Heller, *J. Phys. Chem.* **87**, 4913 (1983).
80. ———, *J. Electrochem. Soc.* **129**, 2865 (1982).
81. C. P. Kubiak, L. F. Schneemeyer, M. S. Wrighton, *J. Am. Chem. Soc.* **102**, 6896 (1980).
82. S. M. Ahmed and H. Gerischer, *Electrochim. Acta* **24**, 705 (1979).
83. D. E. Aspnes and A. Heller, *J. Vac. Sci. Technol.* **B1**, 602 (1983).
84. ———, *J. Phys. Chem.* **87**, 4919 (1983).
85. F. R. F. Fan, R. Keil, A. J. Bard, *J. Am. Chem. Soc.* **105**, 220 (1983).
86. A. Heller *et al.*, *Proc. 15th IEEE Photovoltaic Specialists Conf.* (1981), p. 1722.
87. H. S. Jarrett, A. W. Sleight, H. H. Kung, H. H. Gillson, *Surf. Sci.* **101**, 205 (1980); *J. Appl. Phys.* **51**, 3916 (1980).
88. C. Leygraf, M. Hendewerk, G. A. Somorjai, *J. Catal.* **78**, 341 (1982); *J. Phys. Chem.* **86**, 4484 (1982); *J. Solid State Chem.* **48**, 357 (1983).
89. R. N. Dominey, N. S. Lewis, J. A. Bruce, D. C. Bookbinder, M. S. Wrighton, *J. Am. Chem. Soc.* **104**, 467 (1982); H. D. Abruna and A. J. Bard, *ibid.* **103**, 6898 (1981).
90. J. R. Darwent and G. Porter, *J. Chem. Soc. Chem. Commun.* (1981), p. 145.
91. J. R. Darwent, *J. Chem. Soc. Faraday Trans. 2* **77**, 1703 (1981).
92. D. J. Meissner, R. Memming, B. Kastening, *Chem. Phys. Lett.* **96**, 34 (1983).
93. J. G. Mavroides, D. I. Tchernev, J. A. Kafalas, D. F. Kolesar, *Mater. Res. Bull.* **10**, 1023 (1975).
94. J. G. Mavroides, J. A. Kafalas, D. Kolesar, *Appl. Phys. Lett.* **28**, 241 (1976).
95. T. Watanabe, A. Fujishima, K. Honda, *Bull. Chem. Soc. Jpn.* **49**, 355 (1976).
96. M. S. Wrighton *et al.*, *J. Am. Chem. Soc.* **98**, 2774 (1976).
97. M. A. Butler, R. D. Nasby, R. K. Quinn, *Solid-State Commun.* **19**, 1011 (1976).

98. R. K. Quinn, R. D. Nasby, R. J. Baughman, *Mater. Res. Bull.* **11**, 1011 (1976); K. L. Hardee and A. J. Bard, *J. Electrochem. Soc.* **123**, 1024 (1976).
99. G. Hodes, L. Thompson, J. DeBow, K. Rajeshwar, *J. Am. Chem. Soc.* **105**, 324 (1983).
100. R. A. Simon, A. J. Ricco, D. J. Harrison, M. S. Wrighton, *J. Phys. Chem.* **87**, 4446 (1983).
101. Y. Nakato, A. Tsumura, H. Tsubomura, *Chem. Lett.* (1982), p. 1071.
102. H. Yoneyama, H. Sakamoto, H. Tamura, *Electrochim. Acta* **20**, 341 (1975).
103. A. J. Nozik, *Appl. Phys. Lett.* **28**, 150 (1976).
104. K. Ohashi, J. McCann, J.O'M. Bockris, *Nature (London)* **266**, 610 (1977).
105. A. J. Nozik, *Appl. Phys. Lett.* **30**, 567 (1977).
106. K. Ohashi, K. Uosaki, J. O'M. Bockris, *Int. J. Energy Res.* **1**, 259 (1977).
107. C. Levy-Clement, A. Heller, W. A. Bonner, B. A. Parkinson, *J. Electrochem. Soc.* **129**, 1702 (1982).
108. R. S. Ohl, U.S. patent 2,402,662, filed 27 May 1941, issued 25 June 1946; see also U.S. patent 2,443,542, 17 September 1942.
109. H. Tsubomura, Y. Nakato, A. Tsumura, E. Yoshihiro, *Denki Kagaku Oyobi Kogyo Butsuri Kagaku* **51**, 71 (1983).
110. J. S. Kilby, J. W. Lathrop, W. A. Porter, U.S. patents 4,021,323, 3 May 1977; 4,100,051, 11 July 1978; 4,136,436, 30 January 1979.
111. E. L. Johnson, in *Electrochemistry in Industry*, U. Landau, E. Yeager, D. Kortan, Eds. (Plenum, New York, 1982), pp. 299–306; *Proc. Intersoc. Energy Convers. Eng. Conf.* **16**, 798 (1981); I. Trachtenberg, private communication.
112. A. V. Bulatov and M. L. Khidekel, *Izv. Akad. Nauk SSSR Ser. Khim.* (1976), p. 1902.
113. S. Sato and J. M. White, *J. Am. Chem. Soc.* **102**, 7206 (1980).
114. T. Kawai and T. Sakata, *J. Chem. Soc. Chem. Commun.* (1979), p. 1047; *Chem. Phys. Lett.* **72**, 87 (1980).
115. E. Borgarello, J. Kiwi, E. Pelizetti, M. Visca, M. Graetzel, *Nature (London)* **289**, 158 (1981); *J. Am. Chem. Soc.* **103**, 6324 (1981).
116. J. Kiwi, E. Borgarello, E. Pelizetti, M. Visca, M. Graetzel, *Angew. Chem.* **92**, 663 (1980).
117. J. M. Lehn, J. P. Sauvage, R. Ziessel, *Nouv. J. Chem.* **4**, 623 (1980); *ibid.* **5**, 291 (1981).
118. J. M. Lehn, J. P. Sauvage, R. Ziessel, L. Hilaire, *Isr. J. Chem.* **22**, 168 (1982).
119. E. Borgarello, K. Kalyanasundaram, M. Graetzel, E. Pelizetti, *Helv. Chim. Acta* **65**, 243 (1982).
120. K. Kalyanasundaram, E. Borgarello, M. Graetzel, *ibid.* **64**, 362 (1981).
121. K. Kalyanasundaram, E. Borgarello, D. Duonghong, M. Graetzel, *Angew. Chem.* **93**, 1012 (1981).
122. R. Rosetti, S. Nakahara, L. E. Brus, *J. Chem. Phys.* **79**, 1086 (1983).
123. I thank D. E. Aspnes and B. Miller for valuable discussions and, together with E. A. Chandross and F. H. Winslow, for critically reviewing the manuscript.

RESEARCH ARTICLE

Herbicide-Resistant Mutants from Tobacco Cell Cultures

R. S. Chaleff and T. B. Ray

Abstract. *Several mutants resistant to the herbicides chlorsulfuron and sulfometuron methyl were isolated form cultured cells of* Nicotiana tabacum. *Resistance was inherited as a single dominant or semidominant mutation in all cases. Linkage analysis of six mutants identified two unlinked genetic loci. Studies of plants homozygous for one mutation showed the mutant plants to be completely resistant to treatment with a concentration of chlorsulfuron 100 times higher than that which produces symptoms of phytotoxicity on normal plants.*

In recent years, many novel plant mutants have been isolated by the application of selective growth conditions to cultured cells (*1*). However, few of the variant phenotypes that have been reported so far are of potential agronomic value. This limited practical success of mutant selection in vitro results to a large degree from the genetic and developmental complexity of agronomically important characteristics. Many such traits are exclusively whole plant functions that are not expressed and, therefore, cannot be selected at the cellular level (*2, 3*).

One trait of agronomic interest that may be expressed by cultured cells is herbicide sensitivity. Herbicides that interfere with basic metabolic activities can be expected to inhibit growth of cultured cells as well as of the whole plant. In such cases, herbicide-tolerant mutants can be selected by culturing cells in the presence of a herbicide concentration that is toxic to normal cells. The feasibility of this experimental approach was demonstrated by the isolation of tobacco mutants exhibiting increased tolerance for picloram. Tolerance was expressed by regenerated plants and was transmitted to progeny as a dominant or semidominant nuclear allele (*1, 4, 5*).

We now report the isolation from tobacco cell cultures of mutants resistant to chlorsulfuron and sulfometuron methyl. Chlorsulfuron and sulfometuron methyl (Fig. 1) are, respectively, the active ingredients in the herbicides Glean and Oust (Du Pont). Important features of these compounds are very high herbicidal activities and low mammalian toxicities. The demonstration that chlorsulfuron rapidly inhibits cell division in root tips (*6, 7*) suggested that this herbicide interferes with a basic cellular function and, therefore, could be used to select resistant cell lines in vitro.

Isolation and Genetic Characterization of Mutants

Callus cultures initiated from young leaves of a haploid plant (H1) obtained by culturing anthers of *Nicotiana tabacum* cv. 'Xanthi' (*8*) were maintained on C1 agar medium (*4*). Resistant cell lines were selected by transferring callus to medium supplemented with either chlorsulfuron or sulfometuron methyl at 2 ppb (approximately $5.6 \times 10^{-9} M$). In several experiments, callus cultures were maintained on medium containing 1 m*M* ethylnitrosourea for 3 weeks prior to selection. Isolates C3 and C4 were obtained from cultures that had been mutagenically treated in this manner. Resistant cell lines were propagated on selective medium for two additional passages of 3 weeks each before plants were regenerated as described (*4*). The letter preceding the isolate number indicates the compound on which that isolate was recovered (S for sulfometuron methyl and C for chlorsulfuron).

Crosses of fertile plants regenerated from several isolates were made. The results of crosses with a diploid plant regenerated from isolate S4 (Table 1) demonstrate that the regenerated plant was homozygous for a single dominant nuclear mutation conferring resistance to sulfometuron methyl. Similar series of crosses with plants regenerated from other isolates (S1, S4, S5, S6, S7, C1, C2, C3, C4, and C5) established that, in these cases, resistance likewise resulted from single dominant or semidominant nuclear mutations. Plants regenerated from only one isolate (C3) were heterozygous. Apparently, the mutation conferring resistance on isolate C3 arose after diploidization of a haploid cell of the parental H1 cell line. In all other

---

The authors are on the staff of the Central Research and Development and Agricultural Chemicals Departments, Experimental Station, E. I. du Pont de Nemours & Company, Inc., Wilmington, Delaware 19898.